Electronic Supplementary Material (ESI) for Journal of Materials Chemistry B.
This journal is © The Royal Society of Chemistry 2023

## Supporting Information

# Design of aggregation-induced emission-active fluorogen-based nanoparticles for imaging and scavenging Alzheimer's β-amyloid by photo-oxygenation

Luqi Liu,[a] Wei Liu,[b] Yan Sun,[a] and Xiaoyan Dong*[a]

[a] Department of Biochemical Engineering, School of Chemical Engineering and Technology and Key Laboratory of Systems Bioengineering and Frontiers Science Center for Synthetic Biology (Ministry of Education), Tianjin University, Tianjin 300350, China.

[b] Tianjin Key Laboratory of Radiation Medicine and Molecular Nuclear Medicine, Institute of Radiation Medicine, Chinese Academy of Medical Sciences and Peking Union Medical College, Tianjin 300192, China

*Corresponding authors.

*E-mail address*: d_xy@tju.edu.cn

## Experimental Section

## Materials

1,2-distearoyl-sn-glycero-3-phosphoethanolamine-N-[methoxy(polyethylene glycol)-2000] DSPE-$PEG_{2000}$ and DSPE-$PEG_{2000}$-Mal were purchased from MeloPEG Co., Ltd. (Shenzhen, China). CLPFFD peptides were synthesized by GL Biochem (Shanghai, China). Singlet oxygen sensor green (SOSG) was obtained from Xian Ruixi Biological Technology Co., Ltd. Dihydrorhodamine 123 (DHR 123) was obtained from Glpbio Technology Inc (Montclair, CA, USA). Hydroxyphenyl fluorescein (HPF) was obtained from Shanghai Maokang Biotechnology Co., Ltd. Aβ40 powder with a purity of > 95% was GL Biochem (Shanghai, China). 1,1,1,3,3,3-hexafluoro-2-propanol (HFIP), thioflavin T (ThT), 3- (4,5-dimethylthiazol-2-yl) -2,5-diphenyltetrazolium bromide (MTT), were purchased from Sigma-Aldrich (St. Louis, MO, USA). Fluorescein diacetate (FDA) and propidium iodide (PI) were purchased from DingGuo Biotech. Ltd. (Beijing, China). The cell lines human neuroblastoma SH-SY5Y cells were purchased from Chinese Academy of Sciences (Shanghai, China). Fetal bovine serum (FBS) and Dulbecco's modified Eagle's medium/Ham's F-12 (DMEM/F12) were obtained from Gibco Invitrogen (Grand Island, NY, USA). The wild-type N2 strain and the transgenic CL2006 strain were acquired from the Caenorhabditis Genetics Center, CGC (University of Minnesota, MN, USA). All other reagents with analytical regent grade were purchased from local suppliers.

## Characterization of materials

$^{1}$H NMR spectra were recorded with a JEOL JNM ECZ600R (600 MHz)

spectrometer at room temperature with tetramethylsilane (TMS, δ = 0 ppm) as an internal standard. Fourier transform infrared spectra (FTIR) measurements were performed with an FTIR spectrometer (Nicolet iS50, Thermo Scientific, USA). The morphology of NPs was observed using a field emission transmission electron microscope (TEM) (JEM-2100F, JEOL, Japan). Dynamic light scattering (DLS) measurement was performed using a Malvern Nano ZS instrument at room temperature. UV–VIS absorption spectra were recorded with a spectrometer (Lambda 35, PerkinElmer, USA). A fluorescence spectrometer (Edinburgh FLS1000) was used to record the fluorescence of NPs. Matrix-assisted laser desorption/ionization time-of-flight mass spectrometry (MALDI-TOF MS) experiments were performed with positive ion mode on an Autoflex III TOF/TOF analyser (Bruker Daltonics Inc., Germany) using α-Cyano-4-Hydroxycinnamic Acid as the matrix. The secondary structures of samples were acquired with a circular dichroism spectrometer (J-810, Tokyo, Japan).

**Detection of reactive oxygen species (ROS) generation**

The DCFH-DA was used to detect the ROS generation upon laser irradiation. A reaction system (2 mL) containing 250 μg $mL^{-1}$ of T-LD NPs and 10 μM DCFH-DA reagent was irradiation (660 nm, 72 mW $cm^{-2}$) for different time intervals. The fluorescence change of the solution was measured by excitation at 488 nm and the emission (508-660 nm) was collected. In order to distinguish the type of different ROS generated by NPs, SOSG (Ex: 490 nm, Em: 525 nm), HPF (Ex: 495 nm, Em: 515 nm), and DHR123 (Ex: 495 nm, Em: 525 nm) were used as the indicators to evaluate the

generation of singlet oxygen ($^1O_2$), hydroxyl radical (•OH), and superoxide anion radical ($O_2^{\bullet-}$), respectively. Concisely, SOSG (or DHR123 (10 μM) solution was mixed with the NPs (250 μg mL$^{-1}$) and then irradiated with a laser density of 72 mW cm$^{-2}$. HPF (5 μM) solution was mixed with the NPs (250 μg mL$^{-1}$) and then illuminated under 300 mW cm$^{-2}$ laser. After exposure to laser irradiation, the fluorescence signal of indicator was monitored at different time intervals in the range of 500–600 nm.

**Singlet oxygen detection by electron paramagnetic resonance (EPR) spectrometer**

The ROS generation ability of T-LD NPs was measured by EPR. The 2,2,6,6-tetramethylpiperidine (TEMP) was used as a spin trap agent to detect $^1O_2$, which can react with $^1O_2$ and form a stable radical adduct (2,2,6,6-tetramethylpiperidin-1-yl)oxyl (TEMP-$^1O_2$ or TEMPO). Briefly, 50 μL of TEMP was mixed with 30 μL of T-LD NPs at 250 μg mL$^{-1}$ and irradiated with 660 nm laser (500 mW cm$^{-2}$, 30 min). Similarly, 5,5-Dimethyl-1-pyrroline-N-oxide (DMPO) was used as a spin trap agent to detect ·OH and $O_2^{\bullet-}$. 30 μL of DMPO was mixed with 30 μL of T-LD NPs (250 μg mL$^{-1}$) and irradiated with 660nm laser (500 mW cm$^{-2}$, 30 min). The signals of $^1O_2$, •OH and $O_2^{\bullet-}$ can be record with Bruker EMXplus EPR spectrometer. Meanwhile, T-LD NPs without laser treatment was detected as negative control.

**Aβ monomer/fibril preparation and incubation**

Aβ monomer was prepared according to our previous report.[1] First, The Aβ peptide power was dissolved in HFIP at a concentration of 1 mg mL$^{-1}$. To destroy the pre-existing Aβ aggregates, the solution was kept in quiescence for 2 h and then

sonicated in ice-bath for 20 min. Finally, the HFIP was removed by vacuum freeze-drying (Labconco, MO, USA), and the lyophilized Aβ was stored at -20 °C immediately. Before to use, the treated powder was dissolved in 20 mM NaOH to 275 μM. After being centrifuging at 16,000 g for 20 min at 4 °C, the upper 80% of the supernatant was collected as Aβ monomer and diluted with 100 mM PBS buffer (10 mM NaCl, pH=7.4) for subsequent use. In the inhibition of Aβ aggregation and corresponding cell experiments, 275 μM Aβ stock solution was mixed with different concentrations of NPs to make the final Aβ concentration of 25 μM. In the experiments of disaggregating Aβ40 fibrils, 275 μM Aβ stock solution was diluted with PBS buffer to 50 μM, and then cultured at 37 °C for 4 days to obtain pre-prepared mature Aβ fibrils. The preprepared Aβ fibrils solution was then added to PBS buffer with different concentrations of NPs to the final Aβ concentration of 25 μM.

**Characterization of the binding affinity toward Aβ fibrils**

To confirm the DSPE-PEG-CLPFFD binding affinity toward Aβ fibrils, ThT-labeled Aβ fibrils were dripped and dried on a plate. Then, T-LD NPs were added, followed by incubation for 2 h. The plate was then washed repeatedly and imaged by confocal laser scanning microscopy (CLSM).

**Circular dichroism (CD) spectroscopy**

CD spectra were recorded using a circular dichroism spectrometer (J-810, Jasco, Japan). Aβ sample (400 μL) was added into a quartz cell with a path length of 1 mm, and the ellipticity was recorded at a scanning speed of 200 nm $min^{-1}$. The CD spectrum of Aβ-free solution as the background was subtracted.

**Atomic force microscope (AFM) analysis**

The morphology of Aβ aggregates was recorded using an atomic force microscope (CSPM5500, Benyuan, China) in a tapping mode. To prepare a sample for AFM, a 50 μL of Aβ aggregates was dropped onto a freshly stripped mica flake for 5 min. The salts on mica were removed by gently washing with 5 mL deionized water. The mica substrate was air-dried at room temperature before detection.

**Measurement of photothermal performance of T-LD NPs**

An aqueous solution (20 μg $mL^{-1}$, 1 mL) of T-LD NPs was irradiated by 660 nm laser (power density, 600 mW $cm^{-2}$). The temperature variation during the 20 min irradiation was recorded by a thermal imager (222 s, FOTRIC, Shanghai, China).

**Aβ elimination experiments**

The mature Aβ aggregate solution was added to PBS buffer with different concentrations of NPs to a final concentration of 25 μM. Then, the samples were irradiated by 660 nm laser (600 mW $cm^{-2}$) for 5 min and further incubated for different time. The ThT fluorescence, CD spectrum and AFM images of samples were then acquired after the treatment.

**MTT cell viability**

MTT assay was used to determine the cytotoxicity of T-LD NPs and the inhibitory effects of T-LD NPs on Aβ-induced cytotoxicity. Human SH-SY5Y cells were cultured in DMEM/F12 medium containing 10.0% FBS, 1.0% penicillin–streptomycin antibiotic (100 U $mL^{-1}$ penicillin and 100 U $mL^{-1}$ streptomycin) in a cell incubator at 37 °C under 5% $CO_2$. A total of $8 \times 10^3$ cells/well (80 μL) were seeded into a sterile

96-well plate and cultured for 24 h. Then, 20 μL of aged Aβ solutions (with or without laser irradiation) were added and incubated for an additional 24 h. After that, 10 μL MTT solutions (5.5 μg $mL^{-1}$ in PBS buffer) were added to each well and cultured for 4 h. The culture medium was removed, followed by 100 μL of DMSO was added to dissolve formazan. After shaking at 37 °C for 20 min, the absorbance value at 570 nm was determined with the microplate reader mentioned above.

**Fluorescein diacetate/propidium iodide (FDA/PI) double staining assay**

The alleviation of Aβ-induced cytotoxicity by T-LD NPs was determine using FDA/PI double staining assay. Briefly, a volume of 2 mL SH-SY5Y cells (100,000 cells $well^{-1}$) were seeded into a 6-well plate. After incubating for 24 h, the pretreated Aβ sample in the absence and presence of T-LD NPs was added to the cells and cultured for another 48 h. After removing the culture medium, cells were stained with FDA/PI staining solutions (10 μg $mL^{-1}$ FDA and 5 μg $mL^{-1}$ PI in PBS buffer) for 15 min. Finally, the stained cells were washed five times with PBS and captured with an inverted fluorescence microscope (TE2000-U, Nikon, Japan).

**Statistical analysis**

All data were expressed as mean ± standard deviation (SD). Statistical analyses were determined by one-way ANOVA with Tukey test. Statistical significance was expressed as #$p < 0.05$, ##$p < 0.01$, ###$p < 0.001$, *$p < 0.05$, **$p < 0.01$, ***$p < 0.001$.

**Table S1.** A summary of different photo-oxidant reported in the literatures on the generation of ROS.

| Name | ROS | Reference |
|---|---|---|
| AuNCs@HSA-B | $^{1}O_2$ | 2 |
| Apta@CDs | $^{1}O_2$ | 3 |
| PCN-224 | $^{1}O_2$ | 4 |
| BP@BTA | $^{1}O_2$ | 5 |
| Hf-MOFs | $^{1}O_2$ | 6 |
| bPEI@CDs | $^{1}O_2$ | 7 |
| UCNPs@SiO2-ThS | $^{1}O_2$, •OH | 8 |
| T-LD NPs | $^{1}O_2$, •OH, $O_2^{\bullet -}$ | This work |

**Table S2.** Thermodynamic parameters and binding constants (*K*a) measured by titration of Aβ into T-LD NPs solution.

| | T-LD NPs |
|---|---|
| *K*a ($\times 10^5$ $M^{-1}$) | 2.25 ± 0.67 |
| $\Delta H$ (Kcal $mol^{-1}$) | -36.77 ± 5.48 |
| $T\Delta S$ (Kcal $mol^{-1}$) | -29.38 |
| $\Delta G$ (Kcal $mol^{-1}$) | -7.39 |

**Table S3.** Effects of laser and T-LD NPs (20 μg $mL^{-1}$) on the molecular weight of Aβ monomers.

| Content of different types of Aβ | Aβ (%) | Aβ+1[O] (%) | Aβ+2[O] (%) | Aβ+3[O] (%) | Total oxygenated ratio (%) |
|---|---|---|---|---|---|
| T-LD NPs (-) Laser (-) | 100 | 0 | 0 | 0 | 0 |
| T-LD NPs (+) Laser (-) | 100 | 0 | 0 | 0 | 0 |
| T-LD NPs (-) Laser (+, 10 min) | 100 | 0 | 0 | 0 | 0 |
| T-LD NPs (+) Laser (+, 1 min) | 53.7 | 25.1 | 12.7 | 8.5 | 46.3 |
| T-LD NPs (+) Laser (+, 3 min) | 53.0 | 27.3 | 12.0 | 7.7 | 47.0 |
| T-LD NPs (+) Laser (+, 5 min) | 51.3 | 27.5 | 13.1 | 8.1 | 48.7 |
| T-LD NPs (+) Laser (+, 10 min) | 50.3 | 29.6 | 13.0 | 7.1 | 49.7 |

Oxygenated ratio (%) = (sum of intensities of oxygenated protein)/((intensity of native protein) + (sum of intensities of oxygenated protein)) × 100.

**Table S4.** Effects of laser and T NPs (20 μg $mL^{-1}$) on the molecular weight of Aβ monomers.

| Content of different types of Aβ | Aβ (%) | Aβ+1[O] (%) | Aβ+2[O] (%) | Aβ+3[O] (%) | Total oxygenated ratio (%) |
|---|---|---|---|---|---|
| T NPs (-) Laser (-) | 100 | 0 | 0 | 0 | 0 |
| T NPs (+) Laser (-) | 100 | 0 | 0 | 0 | 0 |
| T NPs (-) Laser (+, 10 min) | 100 | 0 | 0 | 0 | 0 |
| T NPs (+) Laser (+, 1 min) | 77.2 | 10.5 | 5.2 | 7.1 | 22.8 |
| T NPs (+) Laser (+, 3 min) | 71.3 | 14.6 | 6.7 | 7.4 | 28.7 |
| T NPs (+) Laser (+, 5 min) | 66.2 | 17.5 | 8.8 | 7.5 | 33.8 |
| T NPs (+) Laser (+, 10 min) | 64.6 | 21.6 | 8.7 | 5.1 | 35.4 |

Oxygenated ratio (%) = (sum of intensities of oxygenated protein)/((intensity of native protein) + (sum of intensities of oxygenated protein)) × 100.

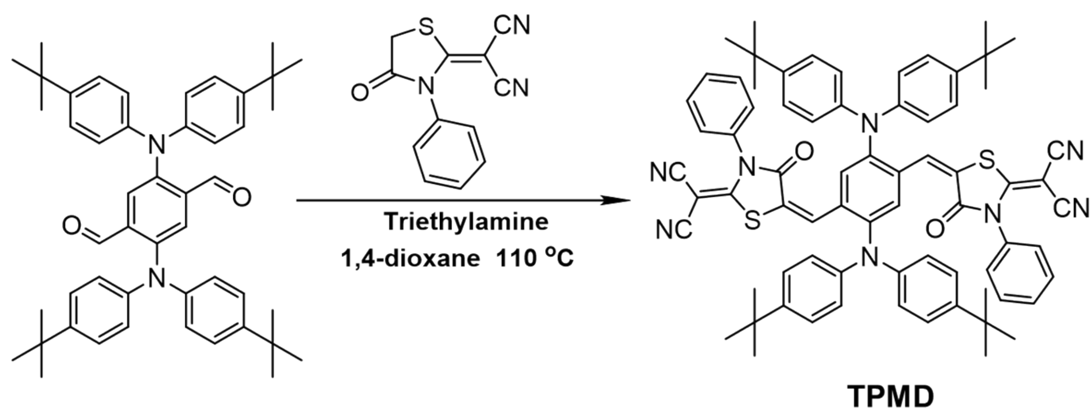


**Fig. S1.** The synthetic route of TPMD.

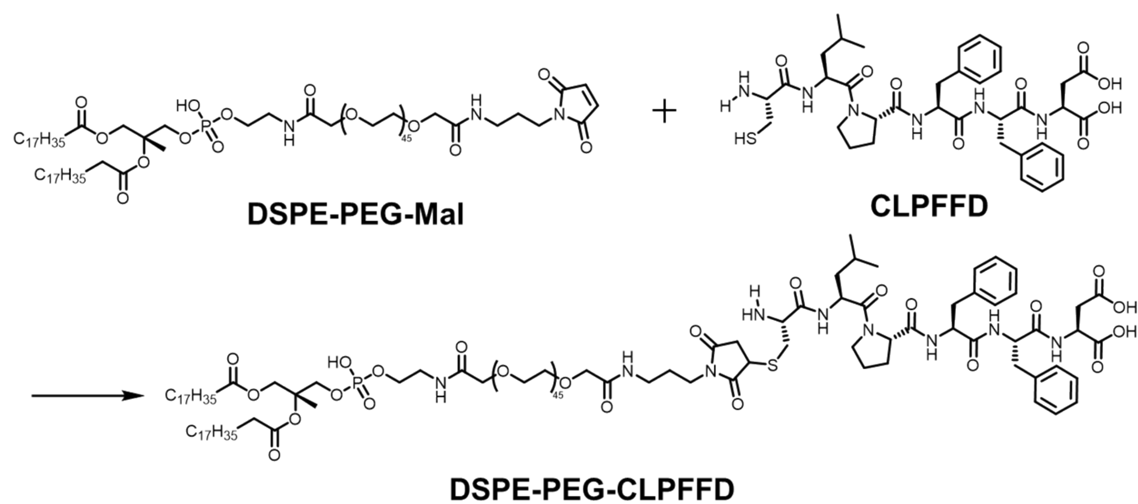


**Fig. S2.** The synthetic route of DSPE-PEG-CLPFFD.

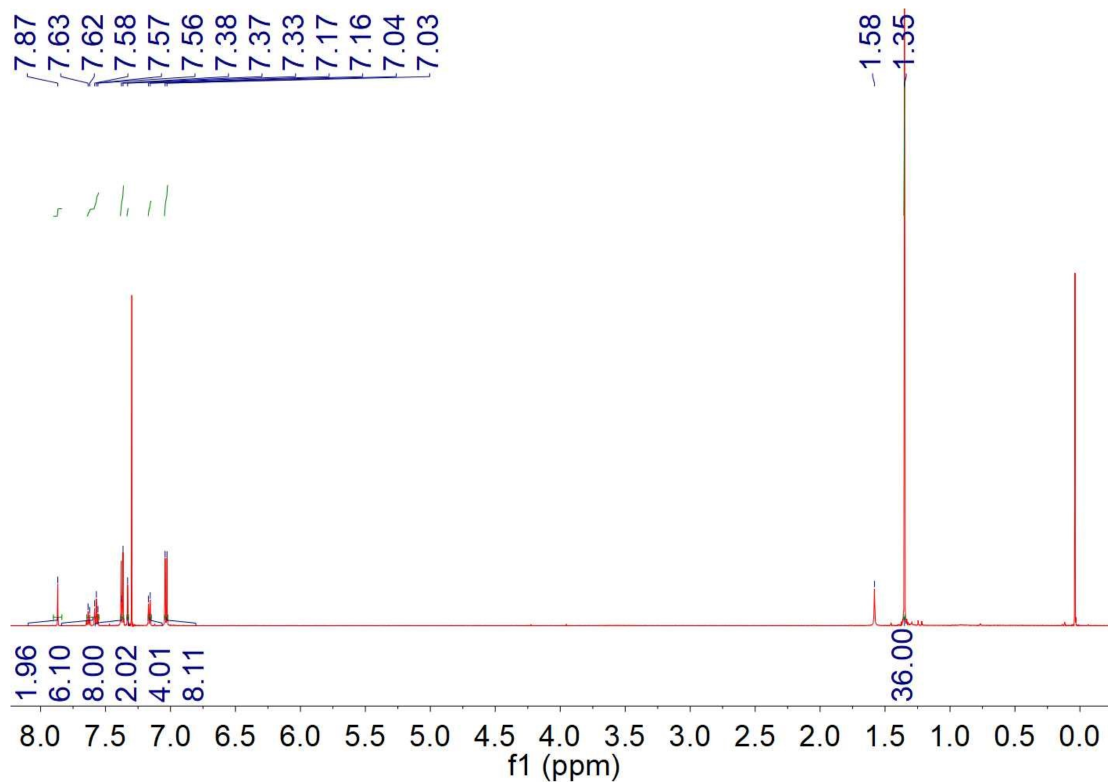


**Fig. S3.** $^{1}H$ NMR spectrum of TPMD in $CDCl_3$.

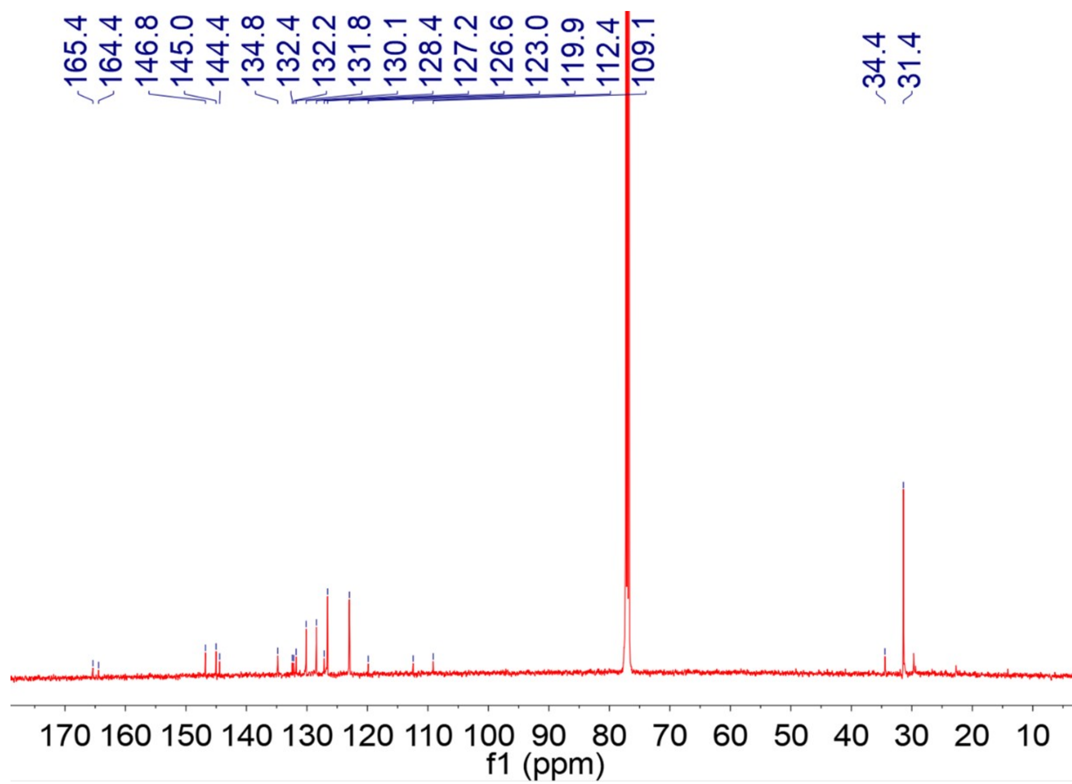


**Fig. S4.** [1]C NMR spectrum of TPMD in $CDCl_3$.

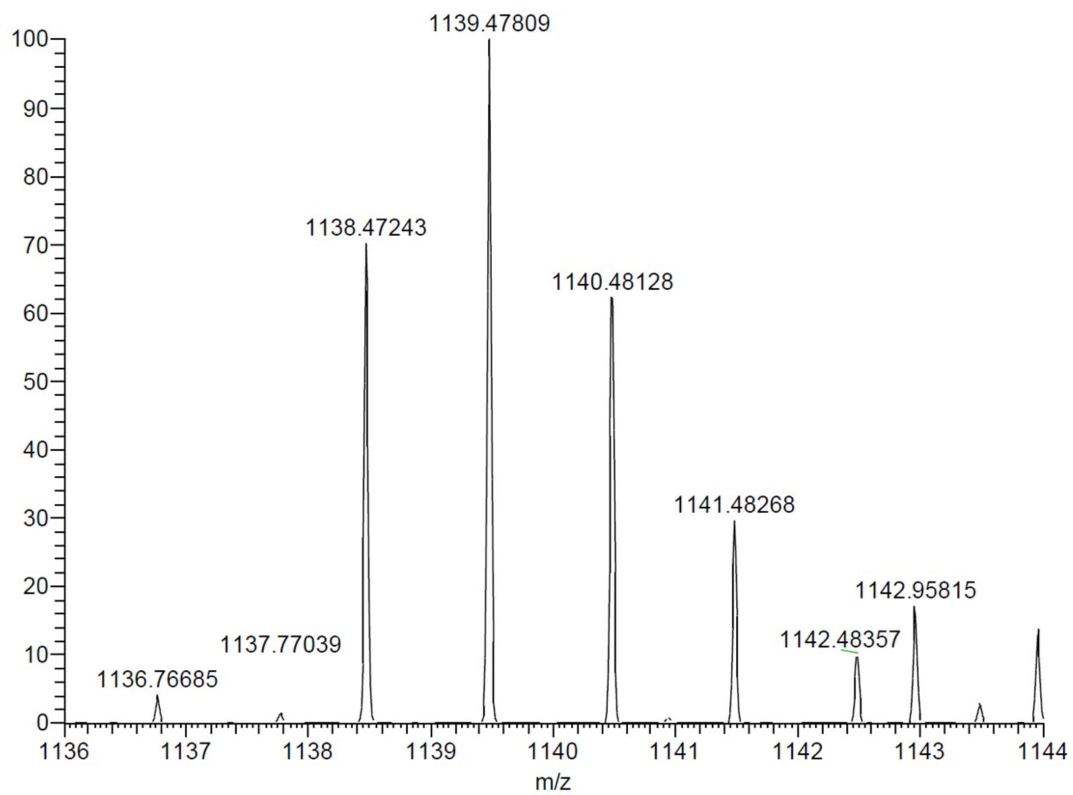


**Fig. S5.** HRMS spectrum of TPMD.

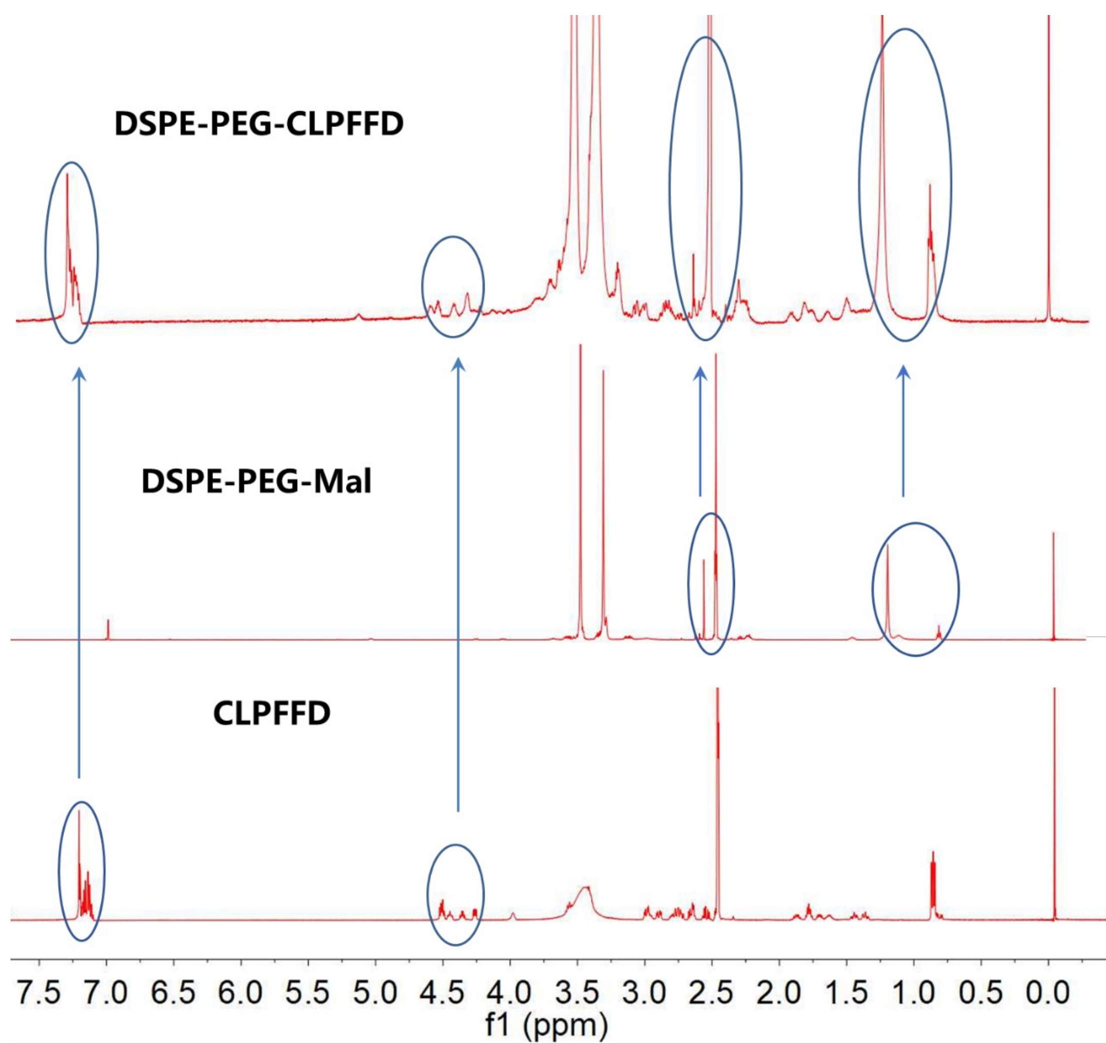


**Fig. S6.** $^{1}H$ NMR spectra of DSPE-PEG-CLPFFD, DSPE-PEG, and CLPFFD in DMSO-d6.

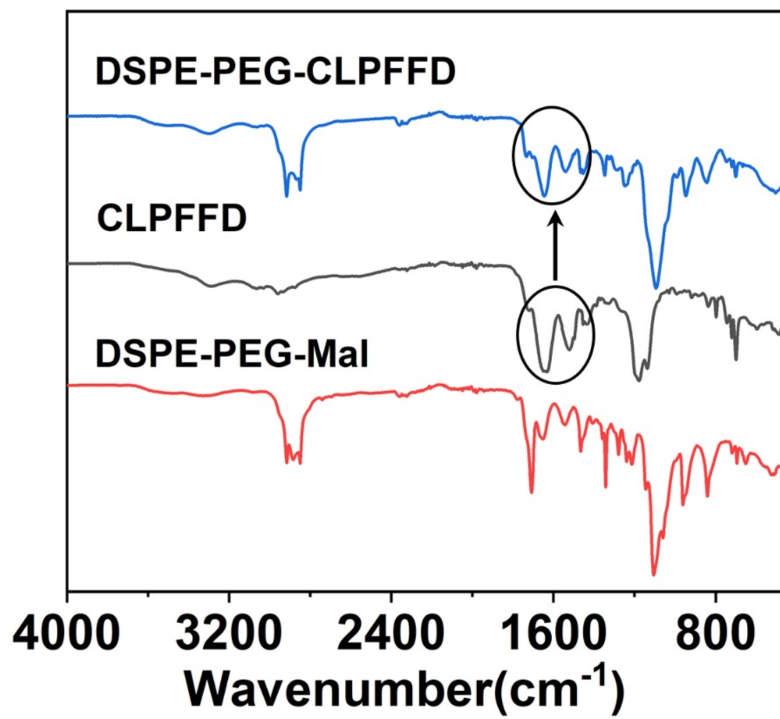


**Fig. S7.** FT-IR spectra of DSPE-$PEG_{2000}$-CLPFFD, DSPE-PEG, and CLPFFD.

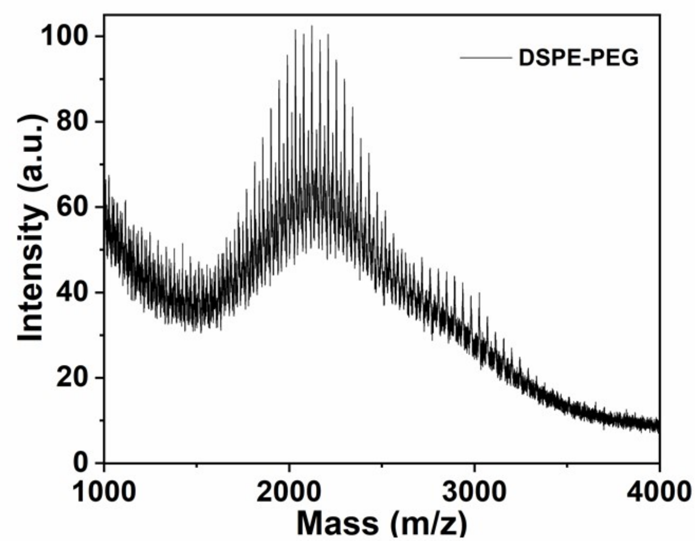


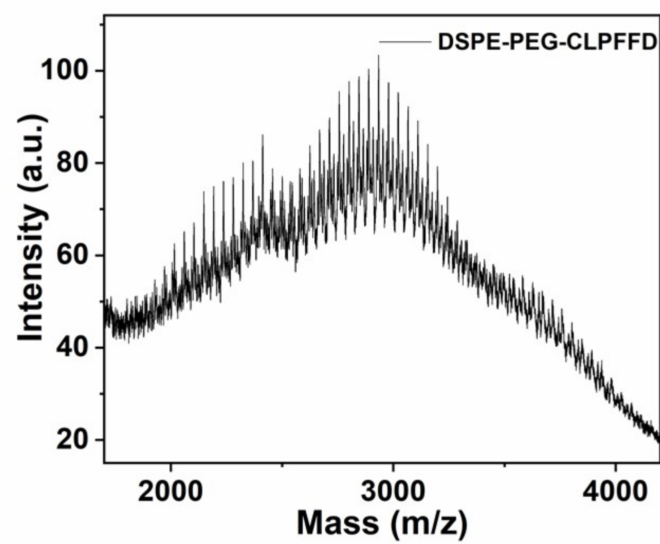


**Fig. S8.** MALDI-TOF spectra of DSPE-PEG and DSPE-PEG-CLPFFD.

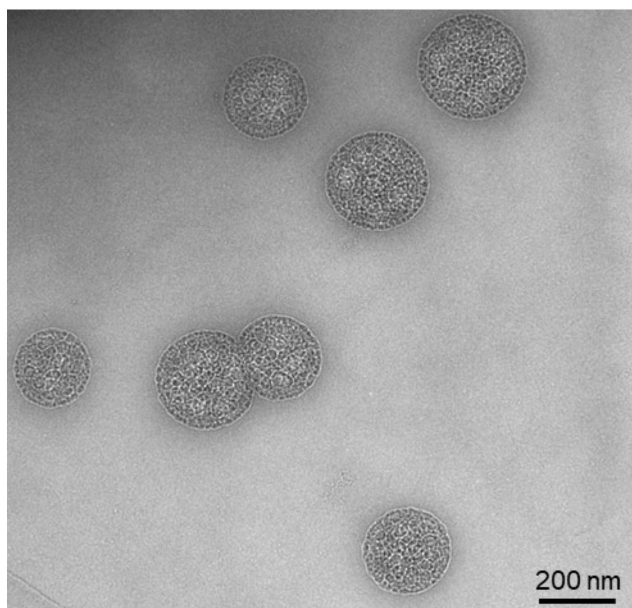


**Fig. S9.** TEM image of T NPs.

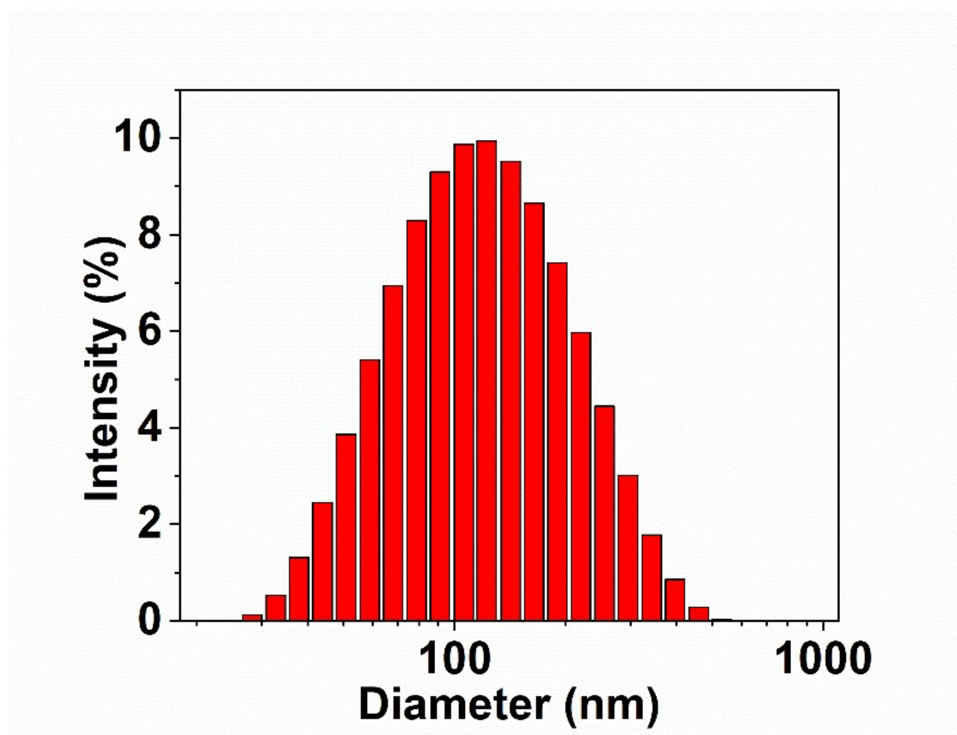


**Fig. S10.** DLS profiles of T NPs.

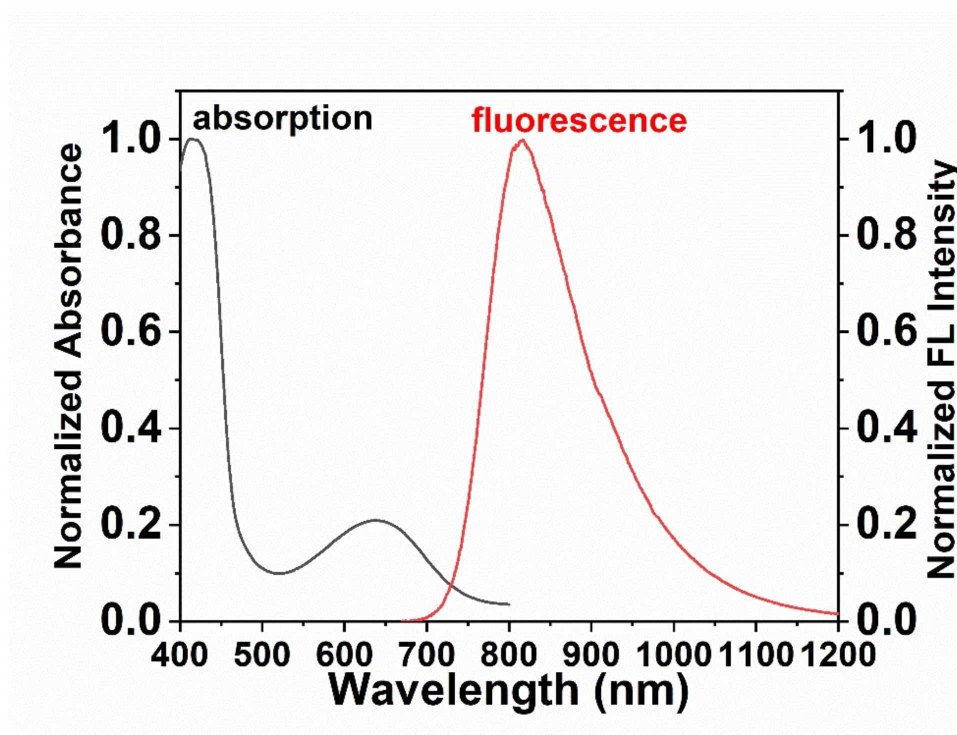


**Fig. S11.** Absorption and fluorescence spectra of TPMD in solid state.

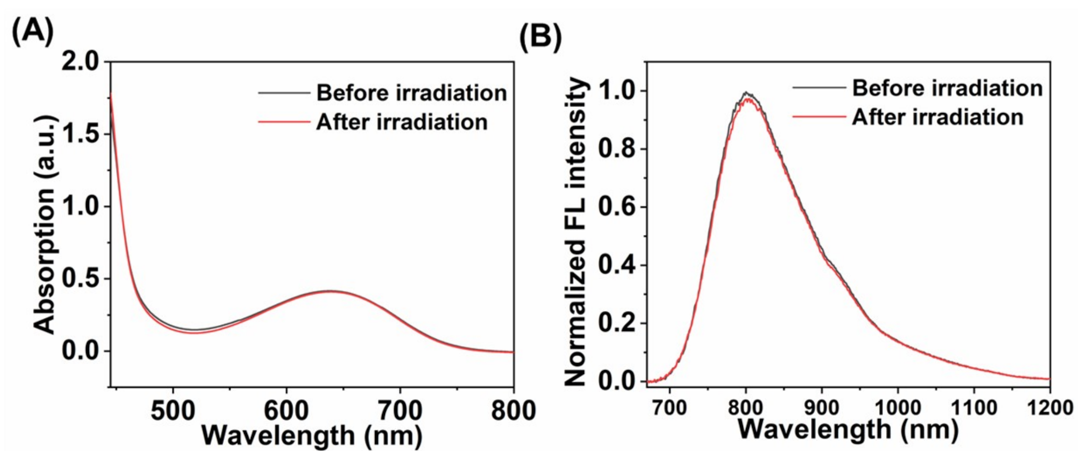


**Fig. S12.** (A) Absorption and (B) fluorescence spectra of T-LD NPs before and after irradiation of 660 nm laser (500 mW $cm^{-2}$) for 20 min.

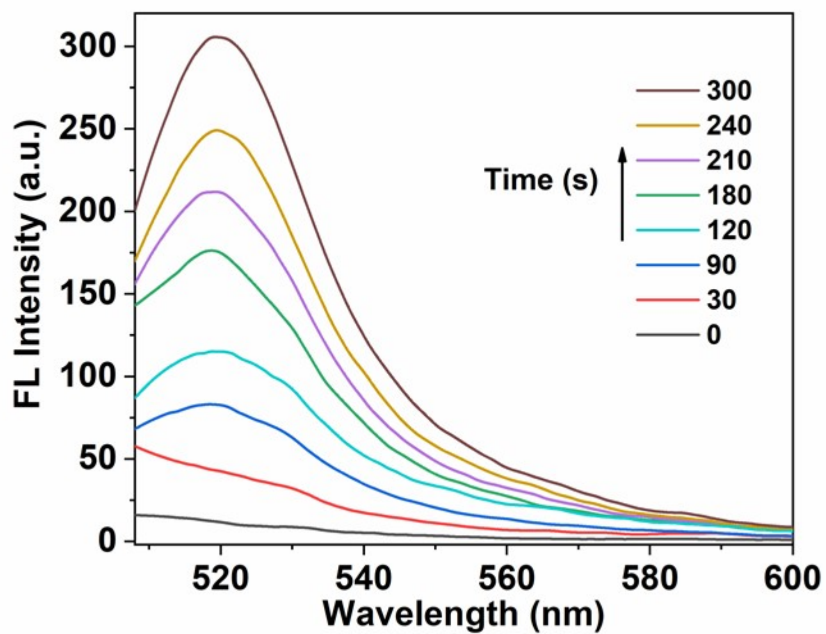


**Fig. S13.** Fluorescence spectra of T NPs (0.25 mg $mL^{-1}$) and DCF-DA (2 μM) in water under laser irradiation for different time (660 nm, 72 mW $cm^{-2}$).

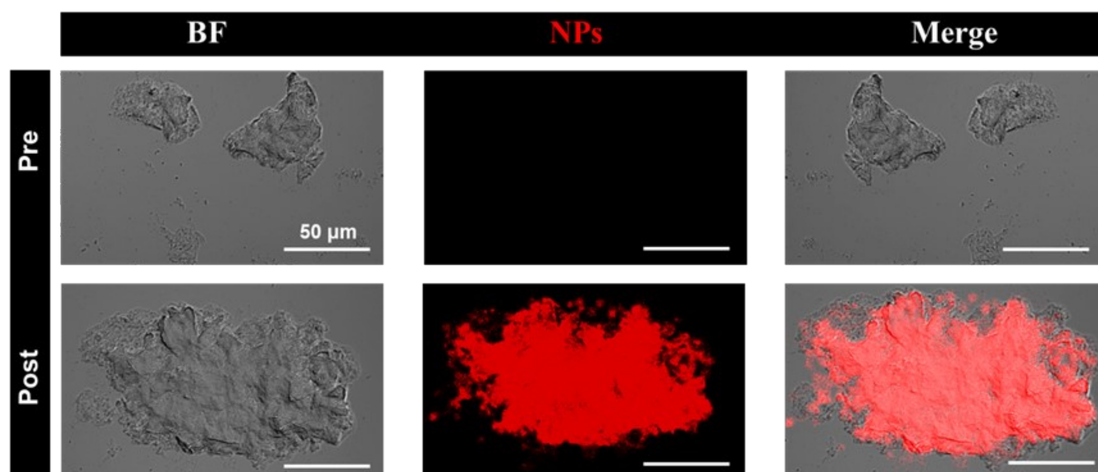


**Fig. S14.** The fluorescence images of Aβ alone (pre) and incubation with T-LD NPs (post), scale bar, 50 μm.

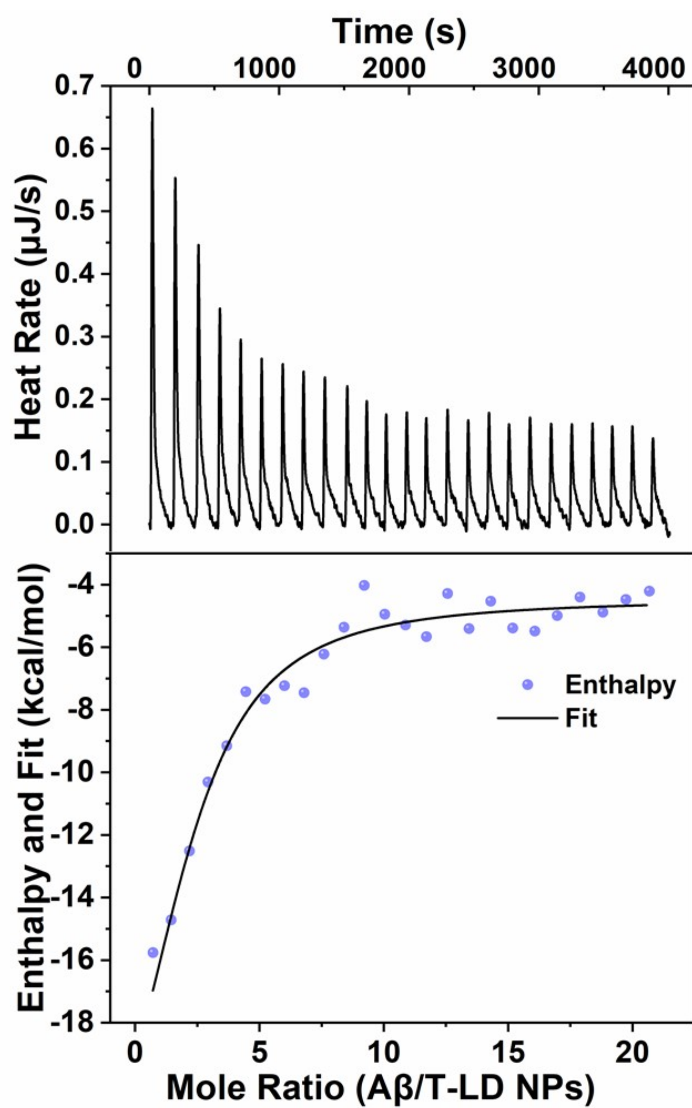


**Fig. S15.** Calorimetric data (raw) for the titration of Aβ (130 μM) into T-LD NPs (20 μM) at 25 °C (top panel). The binding isotherms and the enthalpy values (bottom) were obtained from the integration of raw data in the top panel.

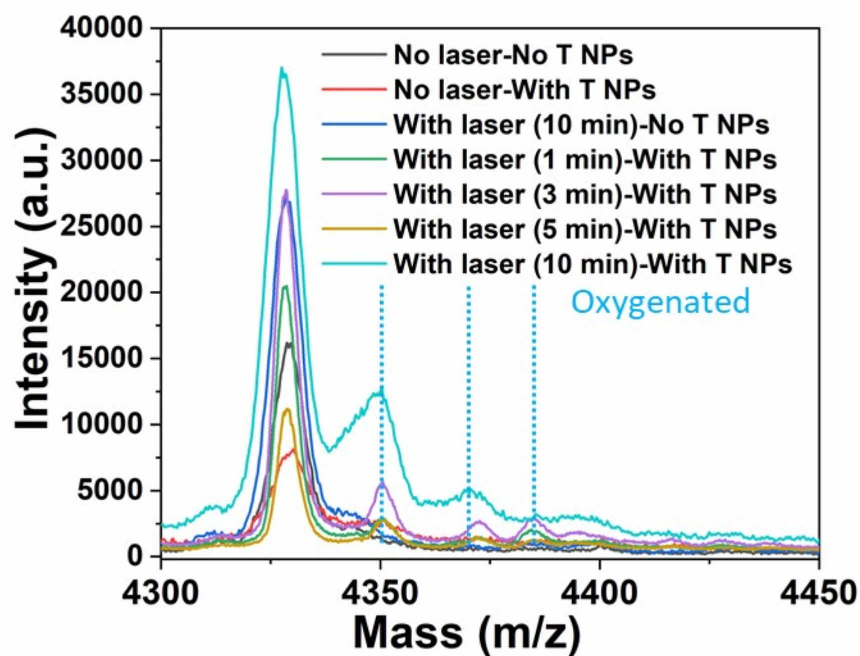


**Fig. S16.** Effects of laser and T NPs (20 μg $mL^{-1}$) on the molecular weight of Aβ monomers (25 μM).

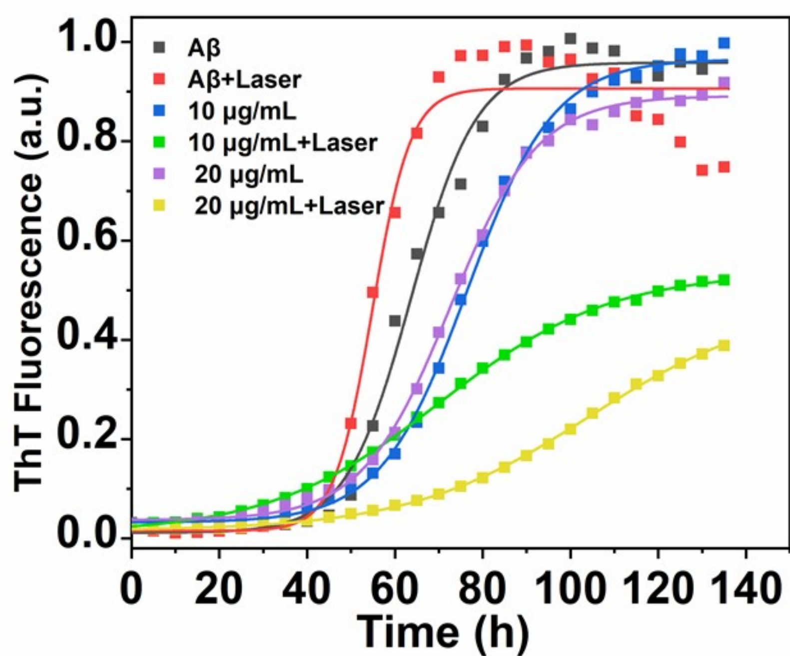


**Fig. S17.** Time-dependent ThT fluorescence changes of Aβ. Aβ (25 μM) containing T NPs was treated with/without laser irradiation (660 nm, 500 mW $cm^{-2}$) for 5 min and then incubated for 140 h.

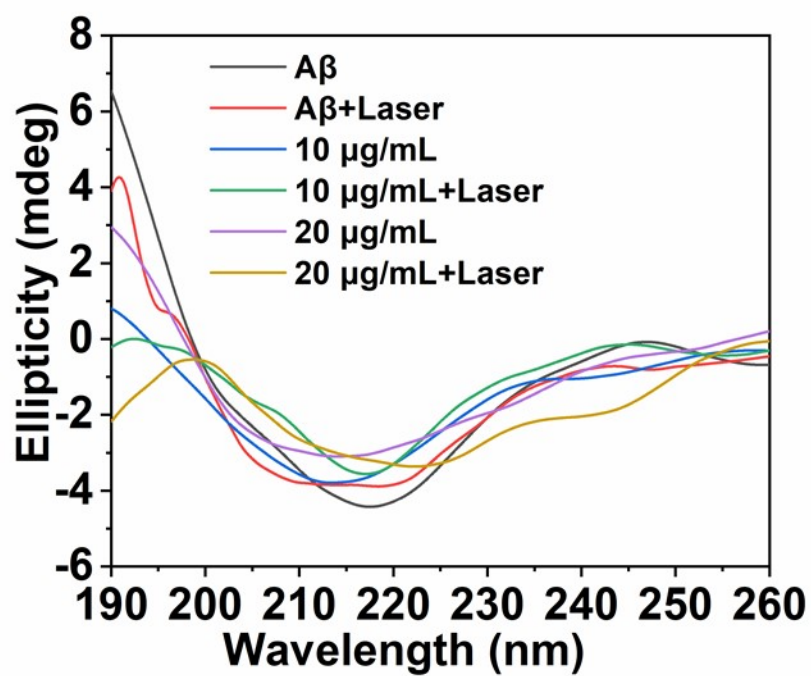


**Fig. S18.** CD spectra of different Aβ samples. Aβ (25 μM) containing T NPs was treated with/without laser irradiation (660 nm, 500 mW $cm^{-2}$) for 5 min and then incubated for 140 h.

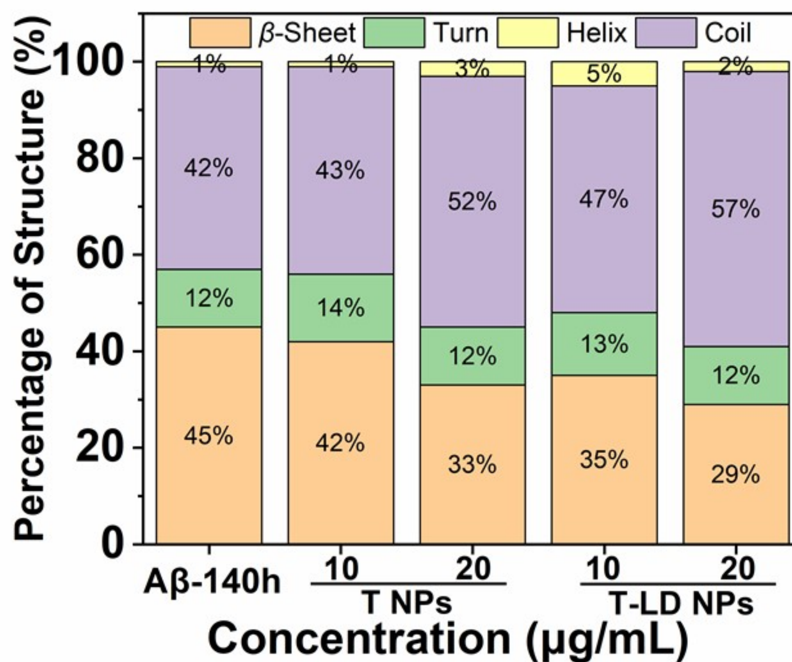


**Fig. S19.** Secondary structure content of different Aβ samples using the Beta Structure Selection (BeStSel). Aβ (25 μM) containing T NPs or T-LD NPs was treated under laser irradiation (660 nm, 500 mW $cm^{-2}$) for 5 min and then incubated for 140 h.

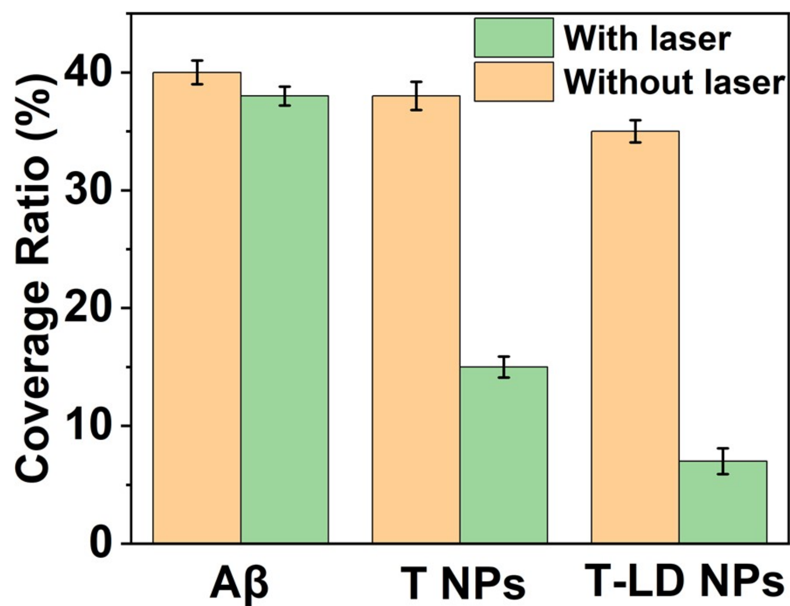


**Fig. S20**. Analyses of the coverage ratio of different Aβ samples. Aβ (25 μM) containing T NPs or T-LD NPs was treated with/without laser irradiation (660 nm, 500 mW $cm^{-2}$) for 5 min and then incubated for 140 h. Each experiment was repeated three times ($n$ = 3); Error bars represent SD.

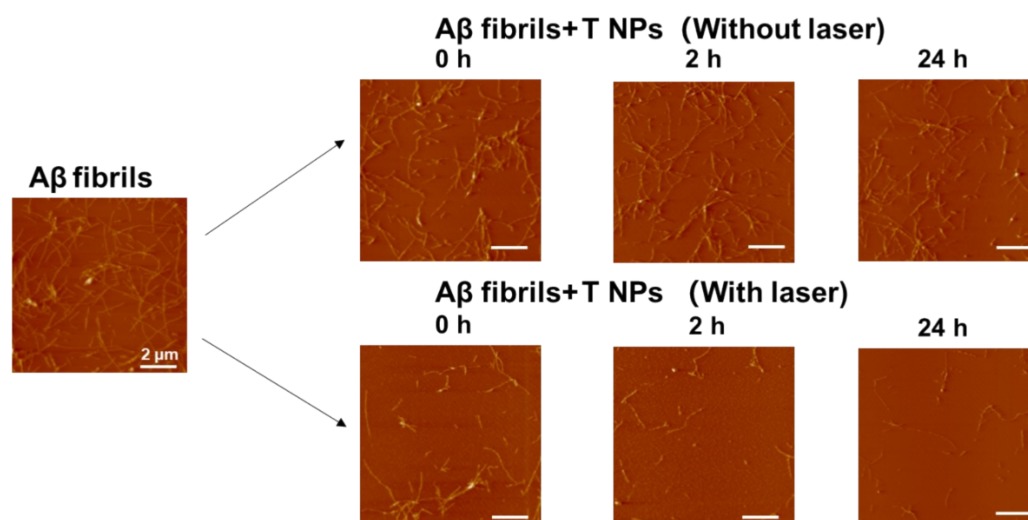


**Fig. S21.** AFM images of Aβ fibrils and Aβ fibrils/T NPs mixtures at different incubation times with/without laser irradiation (660 nm, 500 mW $cm^{-2}$) for 20 min. Scale bar = 2 μm.

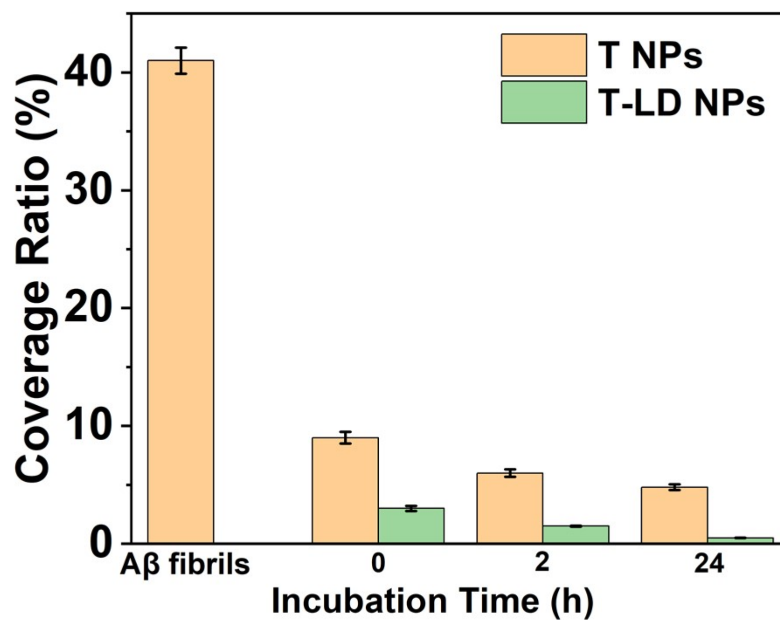


**Fig. S22.** Analyses of the coverage ratio of different Aβ samples. Aβ fibrils and Aβ fibrils/T NPs mixtures at different incubation times under laser irradiation (660 nm, 500 mW $cm^{-2}$) for 20 min. Each experiment was repeated three times ($n$ = 3); Error bars represent SD.

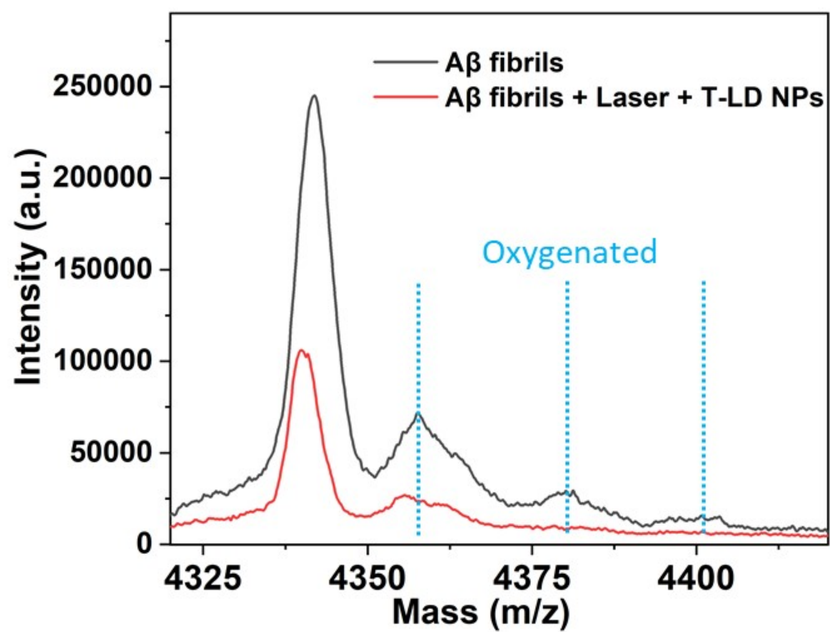


**Fig. S23.** Effects of laser irradiation in the presence of T NPs (20 μg $mL^{-1}$) on the molecular weight of Aβ fibrils (25 μM).

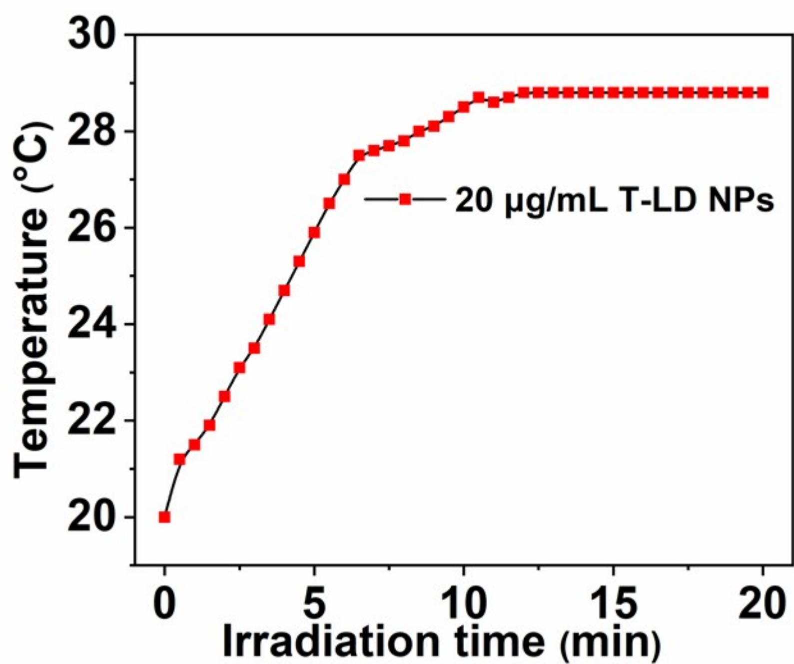


**Fig. S24.** The time course of temperature change of T-LD NPs under laser irradiation (660 nm, 500 mW $cm^{-2}$).

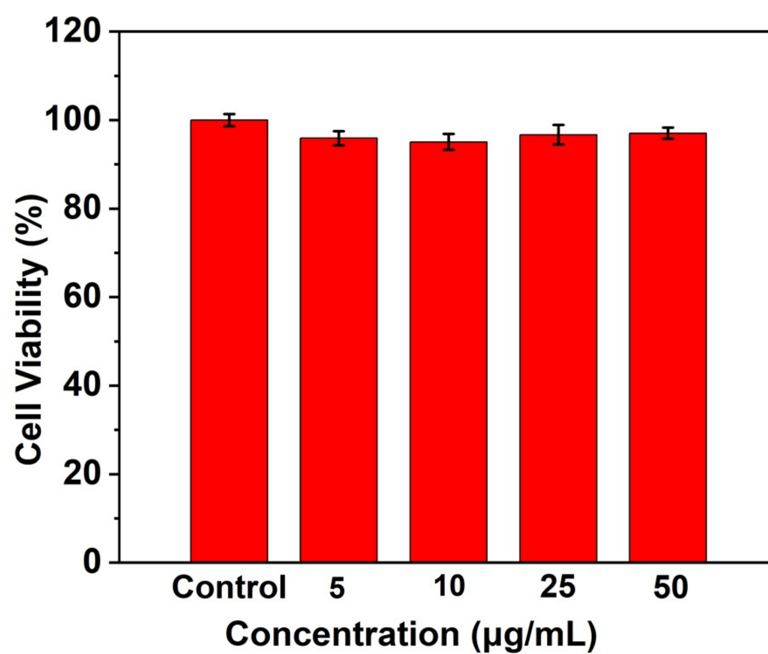


**Fig. S25.** Biocompatibility assessment of T-LD NPs. MTT assay of SH-SY5Y cells treated with different concentrations of T-LD NPs. Each experiment was repeated six times ($n$ = 6); Error bars represent SD.

## References


1 X. Li, W. Wang, X. Dong and Y. Sun, *J Mater Chem B*, 2020, **8**, 2256-2268.

1 W. Liu, H. Zhang, X. Dong and Y. Sun, *Acta Biomater.*, 2022, **144**, 157-167.

2 Y. J. Chung, C. H. Lee, J. Lim, J. Jang, H. Kang and C. B. Park, *ACS Nano*, 2020, **14**, 16973-16983.

3 J. Wang, Y. Fan, Y. Tan, X. Zhao, Y. Zhang, C. Cheng and M. Yang, *ACS Appl. Mater. Interfaces*, 2018, **10**, 36615-36621.

4 Y. Li, Z. Du, X. Liu, M. Ma, D. Yu, Y. Lu, J. Ren and X. Qu, *Small*, 2019, **15**, e1901116.

5 D. Yu, Y. Guan, F. Bai, Z. Du, N. Gao, J. Ren and X. Qu, *Chemistry*, 2019, **25**, 3489-3495.

6 Y. J. Chung, K. Kim, B. I. Lee and C. B. Park, *Small*, 2017, **13**, 1700983.

7 Y. Guan, W. Cao, T. Li, J. Qin, Q. He, X. Jia, Y. Li, Y. Zhang and J. Liao, *J. Mater. Chem. B*, 2023, **11**, 1445-1455.